

Ab initio study of magnetism at the $\text{TiO}_2/\text{LaAlO}_3$ interface

Mariana Weissmann · V. Ferrari · Andrés Saúl

Received: 27 October 2009 / Accepted: 11 January 2010 / Published online: 3 February 2010
© Springer Science+Business Media, LLC 2010

Abstract In this article, we study the possible relation between the electronic and magnetic structures of the $\text{TiO}_2/\text{LaAlO}_3$ interface and the unexpected magnetism found in undoped TiO_2 films grown on LaAlO_3 . We concentrate on the role played by structural relaxation and interfacial oxygen vacancies. LaAlO_3 has a layered structure along the (001) direction with alternating LaO and AlO_2 planes, with nominal charges of +1 and -1, respectively. As a consequence of that, an oxygen-deficient TiO_2 film with anatase structure will grow preferently on the AlO_2 surface layer. We have therefore performed ab initio calculations for superlattices with $\text{TiO}_2/\text{AlO}_2$ interfaces with interfacial oxygen vacancies. Our main results are that vacancies lead to a change in the valence state of neighbor Ti atoms but not necessarily to a magnetic solution and that the appearance of magnetism depends also on structural details, such as second neighbor positions. These results are obtained using both the local spin density approximation (LSDA) and LSDA + U approximations.

Introduction

Thin films of transition metal oxides (ZnO , TiO_2 , HfO_2) were found to be ferromagnetic a few years ago, with a high Curie temperature, when doped with magnetic ions [1–3]. The origin of this magnetic ordering is still debated, but meanwhile ferromagnetism was also found doping with non-magnetic ions, such as Cu [4], and also in undoped cases [5–7]. In order to understand this, several experimental tests were performed in different laboratories: the magnetic ion, the substrate over which the films were grown, the substrate temperature, and the oxygen pressure during film growth were changed. The results are confusing, as some samples are magnetic while others are not [8]. It now seems well established that structural defects, such as oxygen vacancies, and low dimensionality (thin films or nanoparticles) are necessary for the appearance of this type of ferromagnetism [9]. One can understand why it is difficult to obtain reproducible results from different experimental samples, as it is hard to assess quantitatively the influence of defects or disorder in any system.

At the same time, several ab initio calculations have been performed for these oxides in bulk [10–13], with impurities and/or defects, and different models have been proposed to produce the spin ordering. However, few calculations have discussed if surfaces or interfaces have any influence in this type of magnetism [14].

LaAlO_3 (LAO) single crystal is an excellent substrate for epitaxial growth of many oxides, such as SrTiO_3 , BaTiO_3 , PbTiO_3 , and TiO_2 . While the surface electronic structure and atomic relaxation of those oxides [15, 16] and the $\text{SrTiO}_3/\text{LAO}$ interface [17, 18] have been widely studied, the TiO_2/LAO interface has not. In this article, we focus on undoped films of TiO_2 grown on top of an LAO substrate. This system has been found to be ferromagnetic,

M. Weissmann (✉) · V. Ferrari
Departamento de Física, Comisión Nacional de Energía
Atómica, Avda. del Libertador 8250, 1429 Buenos Aires,
Argentina
e-mail: weissman@cnea.gov.ar

V. Ferrari
e-mail: ferrari@tandar.cnea.gov.ar

A. Saúl
Centre Interdisciplinaire de Nanoscience de Marseille, CNRS,
Campus de Luminy, Case 913, 13288 Marseille Cedex 9, France
e-mail: saul@ciman.univ-mrs.fr

with a Curie temperature of about 800 K [6, 7], grown either by pulsed laser deposition or by spin coating. It is also well suited for ab initio calculations because LAO in its cubic phase and TiO_2 in anatase structure, both along the (001) direction, have a very small structural misfit. In fact, thin films of TiO_2 using LAO as a substrate develop anatase structure, indicating epitaxial growth.

The aim of this study is to study the role played by interfacial oxygen vacancies on the magnetic properties of the interface. For this purpose, we consider a model system with a high concentration of vacancies. Under certain conditions, we find a localized magnetic moment in the interfacial Ti atoms, depending not only on the presence of vacancies, but also on the subtle structural details. We do not consider here the possible interaction between these localized moments.

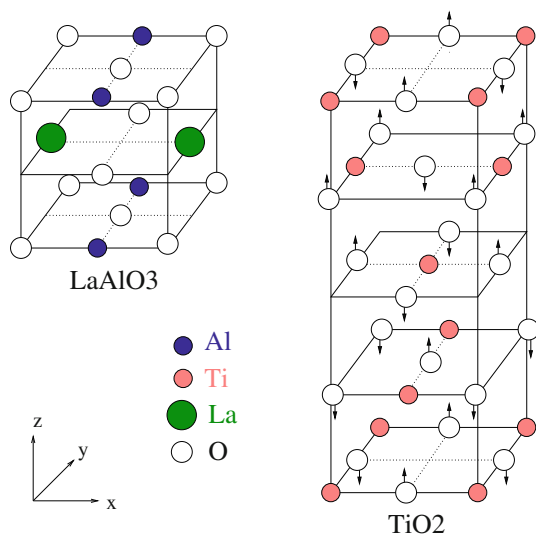


Fig. 1 Unit cells of the two component materials in bulk: LAO (*left*) and TiO_2 anatase (*right*). The *arrows* on the oxygen atoms of anatase indicate the off-plane displacement with respect to the Ti plane

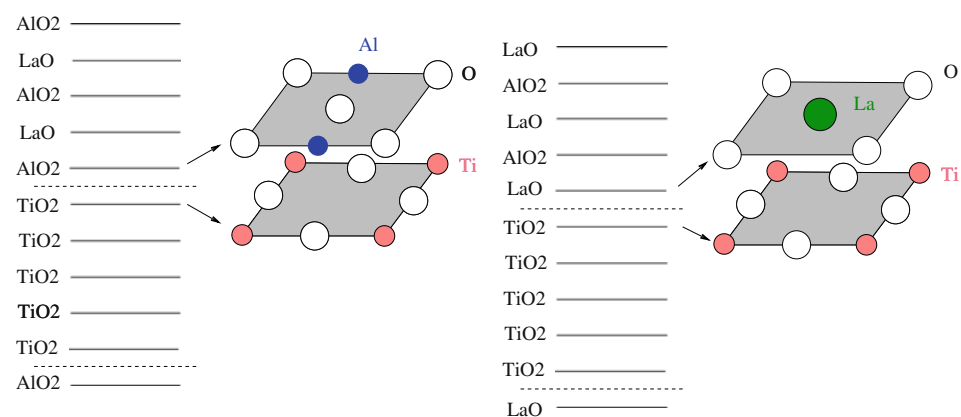
The system

To simulate interfaces, we use a superlattice geometry, so that the system under study results periodic in 3D: ...LAO/ TiO_2 /LAO/ TiO_2 /...

Figure 1 shows the unit cells of the two component materials: LAO and TiO_2 anatase. LAO is a layered material along the (001) direction. The planes LaO and AlO_2 have nominal charges of +1 and -1, respectively. TiO_2 anatase is almost layered: the oxygen atoms are slightly out of the Ti planes, as indicated by the small arrows in Fig. 1. Each plane has zero nominal charge, so that the interface with LAO will restructure due to electrostatics either changing the valence of Ti from Ti^{4+} to Ti^{3+} or Ti^{2+} or by missing oxygen atoms. In this respect, our previous preliminary work [14] showed, using total energy calculations, that it is easier to remove an oxygen atom from the anatase side of the interface than from the LAO side.

Figure 2 shows the two possible interfaces, namely the two ways of stacking to form the superlattice, that maintain the octahedral environment of the Ti atoms. Without oxygen vacancies, our previous calculations [14] showed that neither one has a magnetic solution. With oxygen vacancies near the interface it is clear, due to electrostatics, that the $\text{AlO}_2/\text{TiO}_2$ interface will be preferred with respect to the LaO/TiO_2 one. While there is only one way of stacking in which LaO faces TiO_2 , there are two ways with AlO_2 facing TiO_2 , that we name A and B. They are shown in Fig. 3, that presents the superlattice unit cells used in the present calculations. In order to have all interfaces in the superlattice either of type A or type B, seven anatase planes and five LAO planes are considered. If there are no oxygen vacancies, type A is clearly more stable, with lower total energy, as Al-O bonds are formed at the interface due to the off-plane oxygens in the anatase structure. With oxygen vacancies, each distribution has to be studied separately.

Fig. 2 Schematic diagram of the two possible ways of stacking to form a superlattice: AlO_2 facing TiO_2 (*left*) and LaO facing TiO_2 (*right*). The *dotted lines* indicate the position of the interfaces



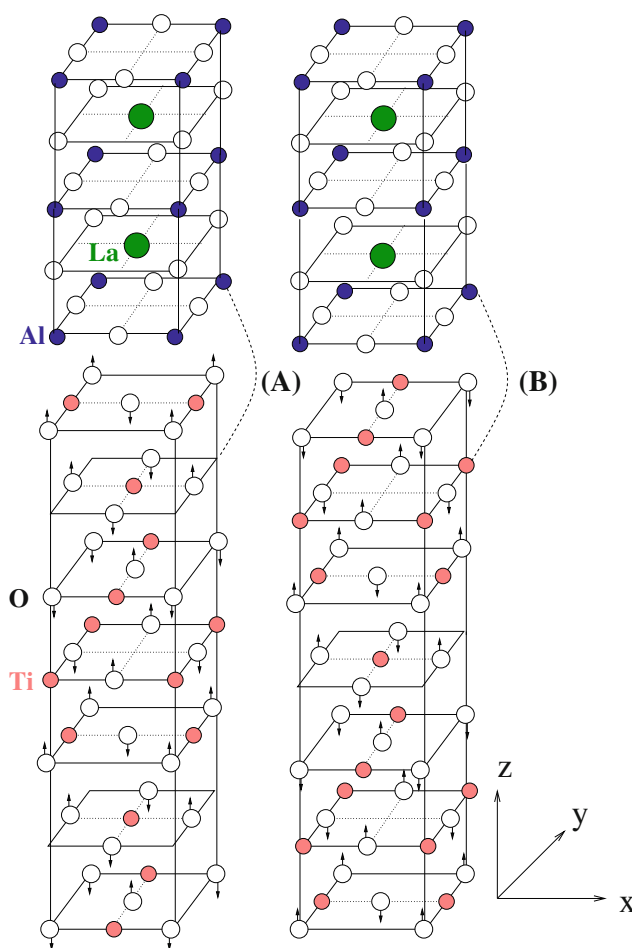


Fig. 3 Unit cells of the two superlattices considered in this study. Due to the off-plane oxygens in the anatase structure and also to the differences in the second neighbor structure (shown by *dotted lines*) there are two types of $\text{AlO}_2/\text{TiO}_2$ interfaces, namely A (*left*) and B (*right*)

The size of the supercells is obtained by minimizing the total energy in each case, and the atomic positions inside the cell are allowed to relax but only in the direction of the superlattice. The reason for this last restriction is based on our previous results, apart from making the calculation more feasible. In fact, the calculations on pure bulk rutile TiO_2 [11] showed that oxygen vacancies can give rise to a local magnetic moment due to structural relaxation. However, this is only true for a fairly large concentration of vacancies and for a fixed cell size, which means there must be some restriction to the full structural relaxation. We could not find a similar result for bulk anatase TiO_2 , but our assumption here is that the LAO substrate could impose such a structural restriction to the anatase film thus giving rise to magnetic solutions. Therefore, the calculations in this article are performed fixing the unit cell size in the direction normal to the stacking to that of cubic LAO

(lattice constant = 3.8 \AA) and relaxation is only allowed in the direction of the superlattice.

Method of calculation and results

For the density functional theory [19] calculations, we have used the Wien2k code [20], that is an implementation of the full potential linear augmented plane waves method, in which the space is divided into muffin tin spheres around the atoms and an interstitial region. Plane waves are used to describe the region outside the spheres. The number of plane waves in the interstitial region is set by the cut-off parameter RK_{max} . In this study, we use $\text{RK}_{\text{max}} = 7$ that corresponds to an energy cut-off of 340 eV. We consider both the local spin density approximation (LSDA) [21] and the LSDA + U [22] one. The calculation is scalar relativistic and the atomic sphere radii are taken to be small, so that the atomic spheres do not overlap when relaxing the structure. They are 1.7 a.u. for Ti and Al, 1.4 a.u. for O, and 2.5 a.u. for La. The number of k -points in the Brillouin zone is 50 or 100 for the relaxation procedure and increased to 200 k -points for the relaxed structure.

Figure 4 shows the densities of states calculated within LSDA for the component systems and for the superlattice. There are no magnetic solutions for any of these cases. The gap obtained for anatase is 2.2 eV, to be compared with the experimental 3.2 eV, whereas the gap for LAO is 4.3 eV, to be compared with the 5.6 eV experimental value. This feature of the LSDA approximation, that gives small band gaps, can be corrected using the LSDA + U method or

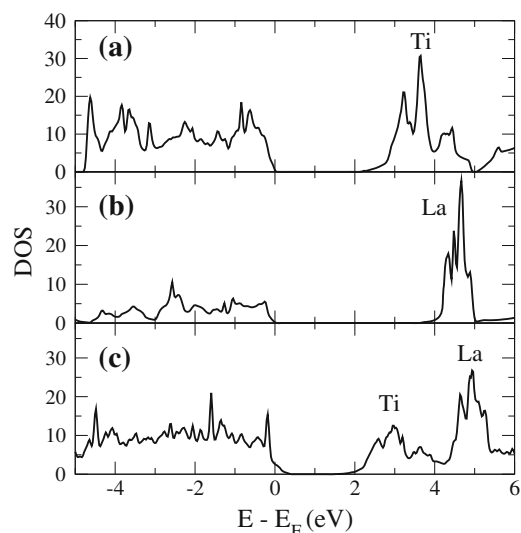


Fig. 4 Calculated densities of states of: *a* bulk TiO_2 anatase, *b* bulk LAO, *c* superlattice with $\text{AlO}_2/\text{TiO}_2$ interfaces (relaxed structure)

hybrid functionals [12]. The LSDA + U approach introduces an additional term based on a simple Hubbard model for electron on-site repulsion. This removes the self-interaction error by energetically penalizing partial occupation of the relevant electronic states, at the price of introducing an empirical parameter in an ab initio calculation.

Before studying the effect of oxygen vacancies at the interface, we start with bulk TiO_2 . Figure 5 shows the densities of states of bulk TiO_2 anatase with one oxygen vacancy in the unit cell, for two different concentrations and both methods of calculation, relaxing all structures

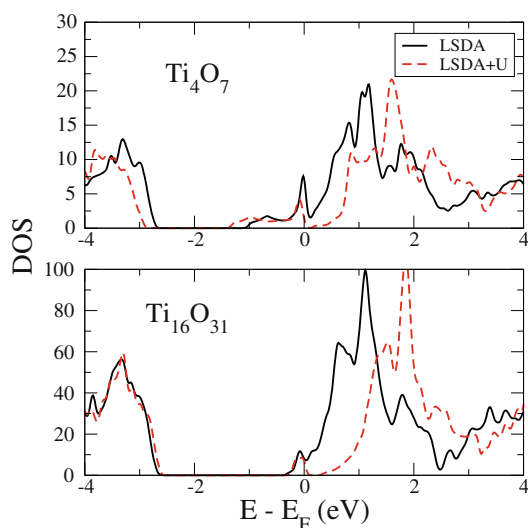


Fig. 5 Calculated densities of states of bulk anatase, with two different concentrations of oxygen vacancies in the LSDA and LSDA + U approximations ($U = 5$ eV). The structure is relaxed separately in each case

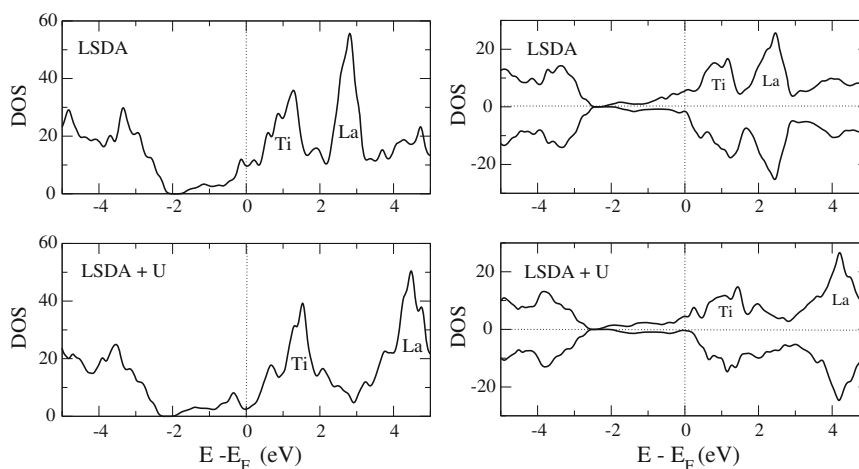


Fig. 6 Calculated densities of states of superlattices A (left) and B (right) shown in Fig. 3 with no oxygen atoms in the Ti side of the interface, using the LSDA (top) and LSDA + U (bottom) approximations ($U = 5$ eV). Case A is not magnetic, so that the contributions

separately. No magnetic solutions are found for any of these cases. A defect state appears inside the band gap, too close to the conduction band in the LSDA approximation, thus making the system metallic. In the LSDA + U approximation, using $U = 5$ eV, the band gap increases by

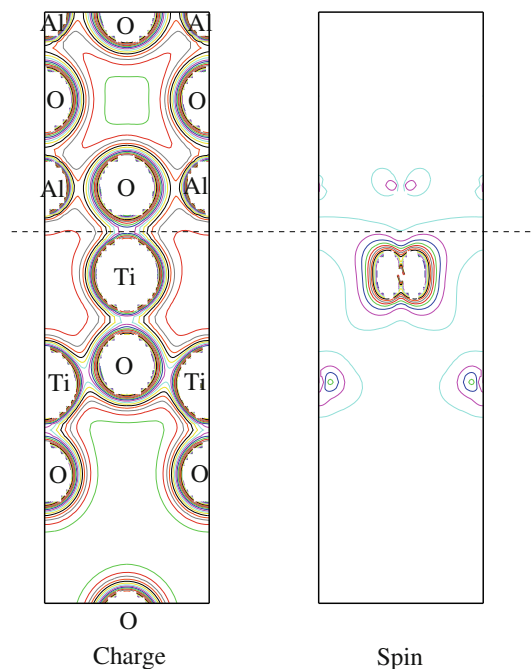


Fig. 7 Charge and spin density maps for superlattice B, near the $\text{AlO}_2/\text{TiO}_2$ interface with two oxygen vacancies. The effect of relaxation is too small to be seen in this scale, but the AlO_2 plane is buckled. Magnetism is mostly localized at the interfacial Ti atom, spin isolines in the figure start at 0.01 and are spaced by 0.03. Charge isolines start at 0.1 and are spaced 0.1. The interface is indicated by a dotted horizontal line

of both spin types have been added. In case B, we show spin up and spin down contributions separately, the magnetic moment of the unit cell is $2.7 \mu_B$ and inside the muffin tin of each interfacial Ti it is $0.65 \mu_B$

about 1 eV and the system becomes a semiconductor, as the defect state is separated from the conduction band. However, using only one parameter U (for the d electrons of Ti), it is not possible to fit both the experimental band gap and the position of the defect state inside the gap (which is at 0.8 eV from the conduction band). It has been shown for reduced rutile TiO_2 surfaces that a discontinuity appears for this property as a function of U at 4 eV and that a larger value is required to insure the semiconductor character of the system as well as the correct position of the gap states [23]. At this point it is important to remark that in this study we consider a large concentration of vacancies in the interfaces, with the defect state developing into an impurity band, and therefore the exact position of the defect state is not so relevant.

Turning now to vacancies at the interface, Fig. 6 shows the densities of states for the supercells A and B of Fig. 3 when all oxygen atoms on the anatase side of the interface have been removed, calculated with LSDA and with LSDA + U . This extreme case is very interesting, as the total energies of systems A and B are equal within the calculation error (1 mRy) but system B is magnetic while

system A is not. The only difference between the two structures lies on the second neighbor layer of the interface, as shown by a dotted line in Fig. 3. The local distortion is similar in both cases, producing a ripple in the interfacial AlO_2 layer.

The magnetic moment in case B is mostly located at the interfacial Ti, as can be seen in Fig. 7. However, the total occupation of the d orbitals in this Ti atom is very similar in cases A and B, both can be considered Ti^{3+} , calculated with LSDA and LSDA + U . In both approximations, the defect level widens to form a band that almost fills the band gap completely, due to the large number of oxygen vacancies. This wide feature inside the band gap is also found in XPS experiments [24].

Discussion and conclusions

The results shown in the previous section call our attention to the following fact: oxygen vacancies lead to a change of valence in a nearby Ti atom turning it into Ti^{3+} , but this does not necessarily imply that the system will have a

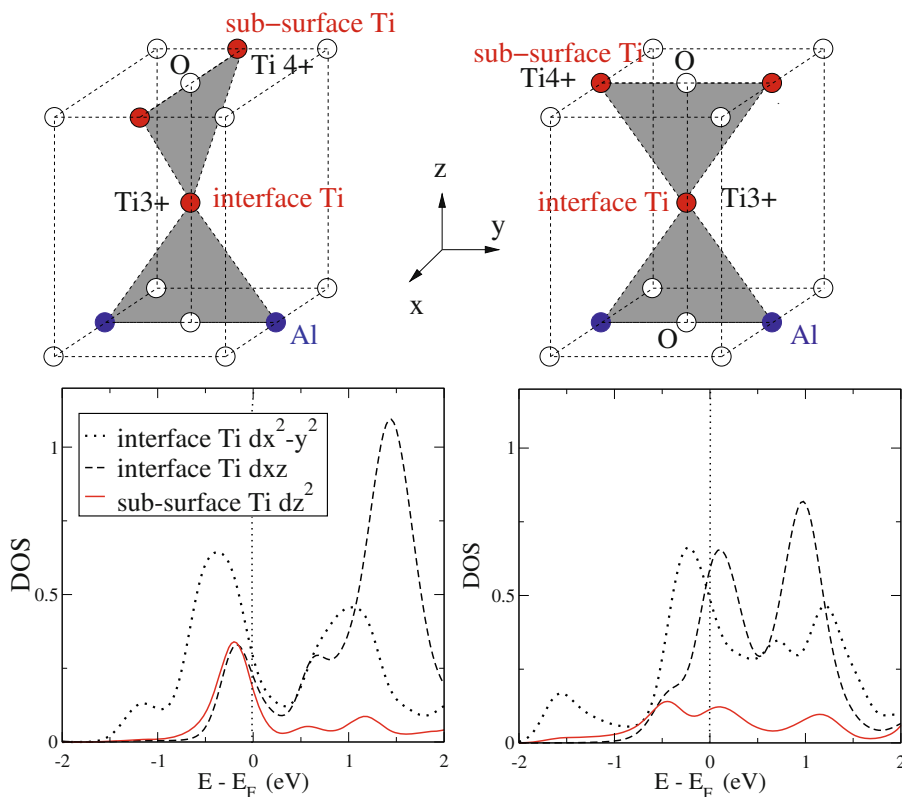
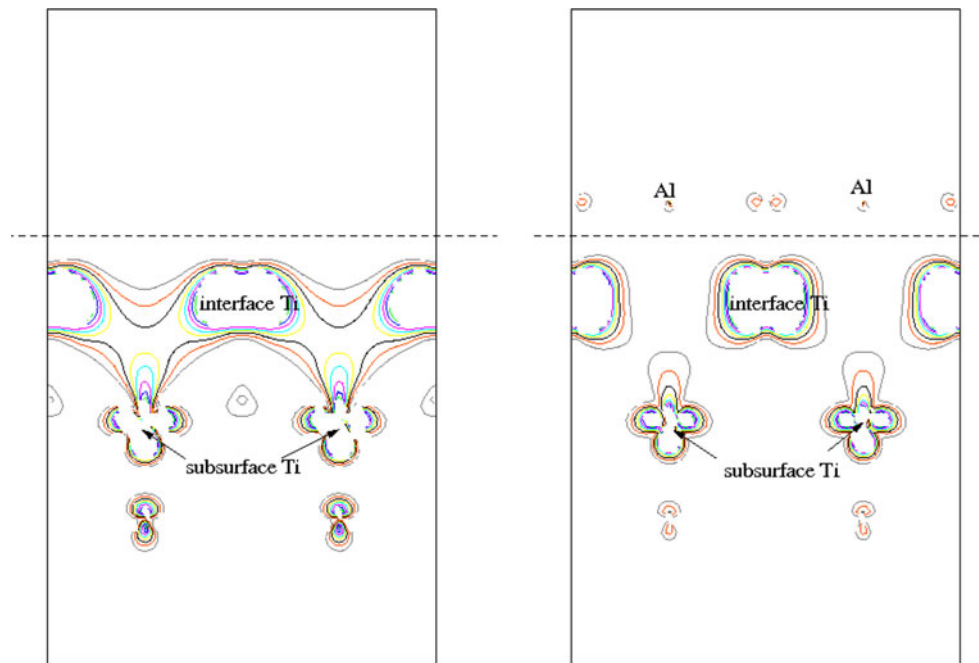


Fig. 8 Non-magnetic calculations for superlattices A (left) and B (right). Top: atomic structures in the proximity of the interfaces. Bottom: local densities of states for an energy range close to the Fermi energy. Dotted line: $d_{x^2-y^2}$ of the interfacial Ti, broken line: d_{xz} of the

interfacial Ti, and full line: d_z^2 of the subsurface Ti atom. Interface A shows a much stronger hybridization (bonding) between orbitals of interfacial and subsurface Ti atoms

Fig. 9 Charge densities at interfaces A (left) and B (right) in the energy range $E_f - 0.5 \text{ eV} < E < E_f$, plotted for yz -plane of Fig. 8. The isolines start at 0.04 and are spaced by 0.02



magnetic solution. In order to understand this unexpected result, we resort to the well-known Stoner criterion. The main idea behind it is that hybridization and band splitting are competing mechanisms to lower the energy of the system. For this purpose, we performed non-magnetic calculations of superlattices A and B, in the unrelaxed structures.

The results are shown in Figs. 8, 9, and 10. The stronger hybridization in case A is quite obvious in Fig. 8: the partial density of states of orbital d_{xz} of the interfacial Ti overlaps

almost completely with that corresponding to orbital d_{z^2} of the subsurface Ti. In case B, the Al atom that is in the same position as the Ti subsurface atom destroys this hybridization. It is the geometric difference in second neighbor positions which drives the system to a magnetic solution.

Another way of looking at this is by plotting the charge density, in an energy range close to the Fermi energy. This is shown in Fig. 9, and as expected it is quite different for both structures.

Figure 10 shows that the non-magnetic total density of states at the Fermi level is larger in case B than in case A, in agreement with the presence of magnetism.

The study of this extreme example, with such a large number of interfacial defects, shows that oxygen vacancies and consequently the presence of Ti^{3+} are a necessary but not sufficient condition to obtain magnetic solutions. This result may be related to the difficulty of producing reproducible experimental results.

Acknowledgement We acknowledge the support by CONICET under Grant PIP 112-200801-38, ANPCyT under Grant PICT-06-157, and a CNRS-CONICET International Scientific Cooperation Project (PICS).

References

1. Matsumoto Y, Shono T, Hasegawa T, Fukumura T, Kawasaki M, Ajmet P, Chikyow T, Koshihara S, Koinuma H (2001) *Science* 291:854
2. Venkatesan M, Fitzgerald CB, Lunney JG, Coey JMD (2004) *Phys Rev Lett* 93:177206
3. Janisch R, Gopal P, Spaldin NA (2005) *J Phys Condens Matter* 17:R657

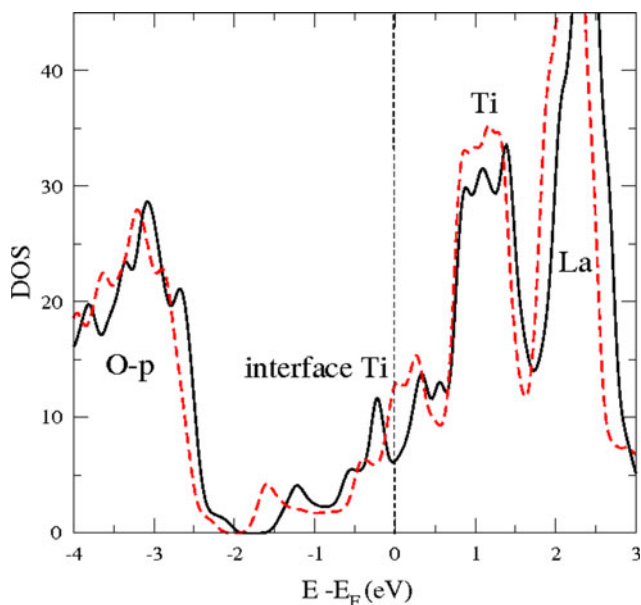


Fig. 10 Calculated non-magnetic total densities of states for superlattices A (full line) and B (dotted line). At the Fermi level, their values are 7.2 for case A and 11.5 for case B, indicating that case B has a larger probability of being magnetic

4. Duhalde S, Vignolo MF, Golmar F, Chilotte C, Torres CER, Errico L, Cabrera AF, Renteria M, Sanchez F, Weissmann M (2005) *Phys Rev B* 72:R161313
5. Venkatesan M, Fitzgerald CB, Coey JMD (2004) *Nature* 430:630
6. Yoon SD, Chen Y, Yang A, Goodrich TL, Zuo X, Ziemer K, Vittoria C, Harris V (2007) *J Mag Mater* 309:171
7. Hassini A, Sakai J, Lopez JS, Hong NH (2008) *Phys Lett A* 372:3299
8. Chambers SA (2006) *Surf Sci Rep* 61:345
9. Sudakar C, Kharel P, Suryanarayanan R, Thakur JS, Naik VM, Naik R, Lawes G (2008) *J Mag Mater* 320:L31
10. Errico L, Renteria M, Weissmann M (2005) *Phys Rev B* 72:184425
11. Weissmann M, Errico L (2007) *Physica B* 398:179
12. Pacchioni G (2008) *J Chem Phys* 128:182505 and references therein
13. Kim D, Hong J, Park YR, Kim KJ (2009) *J Phys Condens Matter* 21:195405
14. Weissmann M, Ferrari V (2009) *J Phys Conf Ser* 167:012060
15. Eglitis RI, Vanderbilt D (2007) *Phys Rev B* 76:155439
16. Eglitis RI, Vanderbilt D (2008) *Phys Rev B* 77:195408
17. Park MS, Rhim SH, Freeman AJ (2006) *Phys Rev B* 74:205416
18. Pentcheva R, Pickett WE (2008) *Phys Rev B* 78:205106
19. Hohenberg P, Kohn W (1964) *Phys Rev* 136:B864
20. Blaha P, Schwarz K, Madsen GKH, Kvasnicka D, Luitz J (2001) WIEN2k, an augmented plane wave + local orbitals program for calculating crystal properties. Karlheinz Schwarz, Techn. Universitt Wien, Austria (ISBN 3-9501031-1-2)
21. Perdew JP, Wang Y (1992) *Phys Rev B* 45:13244
22. Anisimov VI, Solovyev IV, Korotin MA, Czyzyk MT, Sawatzky GA (1993) *Phys Rev B* 48:16929
23. Morgan BJ, Watson GW (2007) *Surf Sci* 601:5034
24. Rumaiz A, Ali B, Ceylan B, Boggs M, Beebe T, Ismat Shah S (2007) *Solid State Commun* 144:334